Semi-empirical Modeling of the Energy Consumed during the Injection Molding Process

Joshua M. Chien and David Dornfeld

Laboratory for Manufacturing and Sustainability, University of California at Berkeley, USA

Abstract

This paper presents a semi-empirical model for determining the energy consumption of an injection molding machine based on the energy profile of the injection molding process. The model utilizes empirical data to the idle or baseline energy consumption of the machine tool, which is non-negligible. A theoretical analysis is used to determine the processing energy, which can be a significant contribution because of the design and the rheological non-Newtonian nature of polymers. A thermo-mechanical analysis of the material plasticizing and injection process is incorporated into the model to accurate assess the theoretical processing energy. The errors in the model are considered and the model performance is validated with findings in literature.

Keywords:

Injection Molding; Semi-Empirical Modeling; Specific Energy Consumption

1 INTRODUCTION

Energy conscious manufacturing has become a reoccurring theme for designers and manufacturers to help lower the environmental footprint of their products by allocating efforts a product's life-cycle, wsignificant emphasis is put on the product's embedded energy. In the case of manufacturing, thorough understanding the energy profile and behavior of the machine tools can allow proper process and material based decisions to be made for reducing the embedded energy. This is crucial in large industries, such as plastics, which is the third largest in the U.S. with market value at over $300 billion [1]. Roughly a third of this value can be attributed to the injection molding market alone, which has a capacity of over 17,000 facilities [1] and install base of over 100,000 injection molding machines (IMMs) [2]. Therefore, improvements to the injection molding processes may have large energy saving implications on the entire plastics industry.

However, obtaining machine tool level energy consumption data can be very time consuming, expensive, and impractical, especially considering the scale of design-of-experiments (DOE) necessary for various materials and under different processing conditions. Therefore, the aim of this research is to create a low cost, comprehensive, and robust injection molding model for accurately predicting the energy consumption of a molded part.

2 BACKGROUND

Plastic IMMs have been used since the turn of the 20th century, with major technological developments occurring from within the last 50 years where parts over 50 pounds and clamp forces exceeding 8000 tons are possible [2].

IMMs can be classified into three categories: hydraulics, all-electrics, and hybrids [3][4]. Hydraulic IMMs are the most mature technological type and utilize pressurized hydraulic cylinders from one or two electric motors and hydraulic pumps to actuate the injection unit and mold clamping. All-electric IMMs represents a relatively new and upcoming technology where electric servo-motors actuate the injection and clamp actuation. All-electrics offer lower power consumption and faster cycle times, but are typically more expensive and limited in the clamp force size. Hybrid IMMs offer the best of both worlds by utilizing the enhancements of all-electric with the addition of hydraulic clamping for high clamp forces. Despite the relatively high new sales of all-electrics and hybrids, hydraulics still represent the largest installed base [2]. Thus, hydraulics will be the primary focus of this paper.

Modeling the energy consumed during injection molding requires detailed understanding of the cycle time behavior and power consumption profile. As shown in Figure 1 the process of injection molding involves many stages where the majority of which occur serially. Post-injection involves parallel stages of plasticizing and part cooling. Note that this type of cycle time behavior represents the majority of thermoplastic (TP) polymers where the material is pre-heated prior to injection and cooled before ejection. Thermoset (TS) polymers are heat treated after injection to cure the polymer in the mold [4]. Due to lack of data, thermoset polymers were not validated in this paper. The generalized IMM power consumption profile is shown in Figure 2; the magnitude of the power in each stage/component will differ depending on the IMM technology and material type.

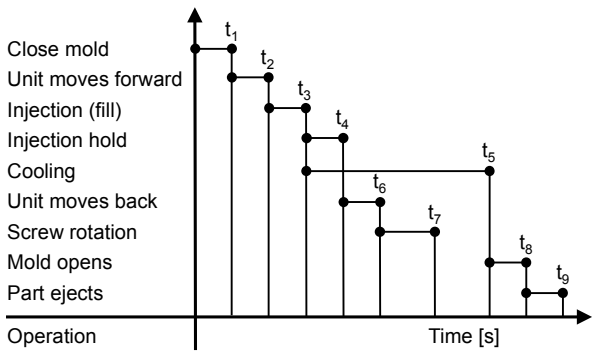

Figure 1: Gate-to-gate cycle time [5].

Power consumption profile can be split into two components: *fixed power*, which represents the idle or baseline power required for machine operation, and *variable power*, which represents machine operations that add direct (e.g. molding) or indirect (e.g. ejection) value to the part [6]. During the operation of a hydraulic IMM, the

fixed power represents the baseline power (e.g. computer, controls), idling stage of the heaters for both the barrel and mold, and the idle running of the hydraulic motor(s), all of which can significantly contribute to the overall energy consumption.

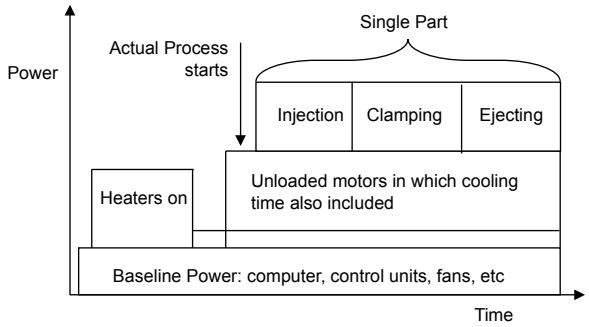

Figure 2: Power characteristics of the injection molding cycle [5].

Past attempts at modeling the energy consumption during injection molding have been well characterized. A common and popular metric is defining a material's *Specific Energy Consumption* (SEC) for a given process [6]. The SEC is essentially the energy required to add, remove, or shape a given mass.

In characterizing the SEC for injection molding, various works in literature have used a theoretical approach while others directly measure the power consumption during molding. Works that model the energy consumption using thermodynamic principles determine the melting energy required and approximate the injection energy as simply the product of the average injection pressure and injected volume [3][7][8][9]. Some have also calculated the power required for screw rotation based on the material's rheological properties [3][8]. The major drawback to the thermodynamic models is that they only encapsulate a small portion of the actual energy consumption. A recent study by Duflou et al. [10] shows that the discrepancy between the thermodynamic models to actual data can range from a factor of 2.4x to over 11.2x.

More representative values for the SEC have been obtained through empirical studies. Qureshi et al. [11] conducted a DOE for mapping out and modeling the SEC of polystyrene. Gutowski et al. [6] and Theriez [3] have collected numerous SEC values for various polymers and different machine sizes and process rates. Ribeiro et al. [7] investigated the influence of part design and calculated the efficacy of the thermodynamic model to the measured data (although the SEC was not directly determined). A more comprehensive study by Weissman et al. [12] took the average measured power consumption of each stage in the molding cycle and their respective theoretical cycle times (with the aid of professional molding software) to obtain an estimate of the total energy per part. While this model took into account tool setup energy and part design, the authors neglected to decouple plasticizing power from cooling power thereby potentially reducing the accuracy of the model.

All the empirical studies that had process parameter variations showed an inverse relationship with SEC to throughput. This trend is due to the higher utilization of the variable energy with respect to the total energy at higher throughputs (the fixed power is relatively constant). However, the trend is mitigated as the machine size (characterized by clamping force) is increased [6], which suggests that the fixed or baseline power does not directly scale proportionally to the size of the machine.

The findings of the empirical studies are useful, but they are often limited in terms of robustness. The reported SEC values apply only to a particular machine size, material, and part design. Mapping out the SEC for the entire family of polymers processed in differently sized machines under a set of throughputs and different geometries would simply be infeasible. Thus, a semi-empirical model that utilizes the strengths of both modeling techniques types may be successful.

3 MODELING

This paper presents a semi-empirical model that is based on theoretical principles and empirical relations. In the previous section, Figure 2 showed the complexity of the injection molding process where numerous stages occur when molding a part. However, since each stage can be considered discrete and virtually independent, superposition can be used to determine the total energy consumption. The SEC then can be constructed as the product sum of the power consumption and time from each stage:

$$SEC = \frac{E_i + E_h + E_r + E_m + E_{moc} + E_b}{TPT\ t_c}$$

$$= \frac{Pt|_i + Pt|_h + Pt|_r + E_m + Pt|_{moc} + (P_b + P_h)t_c}{m_{part}} \quad (1)$$

where E and P denotes the energy and power, respectively, and the subscripts i, h, r, m, moc, b, h, and c denotes the injection energy, hold/pack energy, screw rotation energy during plasticizing, polymer melting energy, mold open/close energy, idle or baseline energy, heater power loss, and cycle time, respectively; TPT is the throughput and m_{part} is the mass of the injected part.

The energy to inject and fill the mold (E_i) and the energy for melting (E_m) and plasticizing (E_r) is highly material dependent and can be explicitly modeled using thermo-mechanical principles. The remaining stages are difficult to explicitly model due to their high dependence on the machine size and manufacturer's design. Therefore, an empirical approach is used to generalize the actual power consumption during idling, holding, and mold opening/closing with respect to machine size. The following few sections will describe in detail each stage of model.

3.1 Thermo-Mechanical Model

The power required to inject the molten polymer is a function of the volumetric flow rate and the hydraulic pressure loss [13]. Taking account the efficiency of the motor and hydraulic pump, the power delivered to the electric motor can be written as:

$$P_i = Q\frac{dP_t}{\varepsilon_M \varepsilon_h} \quad (2)$$

where Q is the volumetric flow rate entering the mold, dP_t is the total pressure loss in the mold, ε_M is the electrical efficiency of the motor (which is dependent on the motor size), and ε_h is the hydraulic efficiency of the pump. The total pressure loss can be further calculated as the sum of the channel pressure losses:

$$dP_t = dP_s + dP_r + dP_{mo} \quad (3)$$

where dP_s, dP_r, dP_{mo} are the channel pressure losses of the sprue, runner, and mold, respectively. Due to the non-Newtonian viscoelastic behavior of the molten polymer the channel pressure loses are modified to yields the following equation (for the mold) [13]:

$$dP_{mo} = \frac{ML_{mo}}{H_{mo}}\left[\frac{2Q(1/n+2)}{W_{mo}H_{mo}^2}\right]^n \quad (4)$$

where L_{mo}, H_{mo}, and W_{mo} are the channel length, height, and width of the mold, respectively. The parameters M and n are coefficients derived from the non-Newtonian viscosity and shear rate model (see Section 3.4). Similar equations hold for the sprue and runner.

The power required for screw rotation and plasticizing is highly dependent on the screw design, size, rotational speed, and the shear temperature dependent viscosity. The equation for plasticizing power delivered by the electric motor is given by [13]:

$$P_r = \bar{\mu}(\dot{\gamma},T)\frac{\pi^2 N^2 D_b^2 WL}{sin\,\bar{\theta} H \varepsilon_M}\left(4 - 3\,cos^2\,\theta_b \frac{Q_{ex}}{Q_d}\right) \quad (5)$$

where $\bar{\mu}(\dot{\gamma},T)$ is the average viscosity at shear rate, $\dot{\gamma}$, and temperature, T; N is the screw speed, D_b is the screw diameter, W is the screw channel width (distance between flights), H is the screw channel height, L is the screw length, $\bar{\theta}$ is the average screw helix angle, θ_b is the screw helix angle at the barrel surface, Q_{ex} is the volumetric rate exiting the screw, and Q_d is the volumetric flow rate that is dragged by the screw. Note that $0 \le Q_{ex} \le Q_d$ and when $Q_{ex} = 0$ (i.e. when the shot volume is full) the rotational power is at its maximum, and when $Q_{ex} = Q_d$ (i.e. open flow) the rotational power is at its minimum.

While the shearing during plasticizing may generate some heat, barrel heaters are needed to melt the polymer and to reach proper injection temperatures. The additional thermodynamic energy required depends on the polymer's crystalline structure and can be determined by the following equation [3]:

$$E_m = mc_p\left(T_i - T_{hop}\right) + \lambda m H_F^o \quad (6)$$

where m is mass of the shot, c_p is the average specific heat capacity, T_{inj} is the injection temperature, T_{hop} is the polymer temperature in the hopper, λ is the average degree of crystallinity (note crystallinity decreases with temperature), and H_F^o is the average heat of fusion at 100% crystallinity. For amorphous polymers, λ is set to zero.

Equation 6 describes the minimum energy required to melt the polymer. However, in reality there are conductive heat losses primarily through the barrel, screw, and mold. The heat losses are heavily dependent on the machine size and design, and while a proper heat transfer analysis is beyond the scope of this study, the analysis can be simplified by assuming natural or free convection as the primary means of heat dissipation. Therefore, the equation for the heat loss is given by:

$$P_h = \left(P_{heat,b} + P_{heat,p}\right)/\eta_{heat} \quad (7)$$

where $P_{heat,b}$ and $P_{heat,p}$ are the convective heat loss (in Watts) for the barrel and mold platen, respectively. The η_{heat} term is designated to be the ratio of the convective heat loss to the total loss; hence $1 - \eta_{heat}$ represents the conductive and radiative heat losses. The convective heat loss of the barrel can be modeled as a cylinder where the outer diameter is the characteristic length, which is assumed to be 2.5 times that of the barrel diameter. The equation is expressed as [14]:

$$P_{heat,b} = \pi\, Nu_D\, k_{air}\, L_b\, (T_i - T_{amb}) \quad (8)$$

where k_{air} is the thermal conductivity of air at the average temperature, L_b is the length of the barrel and is assumed to be equal to the screw length, T_i is the injection temperature (in reality the barrel surface temperature is less than the injection temperature due to insulation of the barrel), T_{amb} is the ambient air temperature and is assumed to be 20°C. The term Nu_D is the Nusselt number, which is the ratio of the convective to conductive heat transfer across the barrel [14] and is approximated as:

$$\boldsymbol{Nu_D = 0.48\, Ra_D^{0.25} \qquad 10^4 \le Ra_D \le 10^7} \quad (9)$$

where Ra_D is the Rayleigh number, which describes the ratio of the free convective flow to the thermal diffusivity. The Rayleigh number is also defined as the product of the Grashof and Prandtl numbers and can be written as [14]:

$$\boldsymbol{Ra_D = \frac{g\,\beta\,(T_i - T_{amb})\,(2.5\,D_b)^3}{\nu_{air}\,\alpha_{air}}} \quad (10)$$

where g is the grativational accerlation (9.81m/s^2), β is the coefficient of volume expansion and is taken as the inverse mean temperature, $2.5D_b$ is the outer barrel diameter, ν_{air} and α_{air} is the kinematic viscosity and thermal diffusitivity of air at the average temperature, respectively. The natural convective heat loss for the mold platen can be calculated in a similar manner where the characteristic length is the platen height and the heat transfer profile is assumed to be that of a vertical wall.

3.2 Empirical Model

A meta-analysis from various empirical studies of the injection molding power consumption profiles was conducted to construct the models for the idle or baseline (P_b), clamp hold (P_h), and mold open/close (P_{moc}) power consumptions. Various profiles involving different machine sizes were publically found in literature and analyzed. Figure 3 shows an example profile of polystyrene with a 15-ton injection molding machine [11]. Power consumptions of each stage in the profile were approximated as accurately as possible.

The results of the meta-analysis showed very high correlations between the idle, hold, and open/close power consumption to machine size. It was observed that the best fit for idle and holding power consumptions was linear while the mold opening and closing fit was exponential. Fitting other stages such as injection and plasticizing was also attempted, but no clear correlations could be made as expected.

From the empirical data, the models were formulated using linear regression (log-linear for exponential curves) and the coefficients of the slope, m, and y-intercept, b, are calculated using the equations:

$$m = \frac{N\sum_{j=1}^{N}\left(T_j P_j\right) - \sum_{j=1}^{N} T_j \sum_{j=1}^{N} P_j}{N\sum_{j=1}^{N}\left(T_j^2\right) - \left(\sum_{j=1}^{N} T_j\right)^2} \quad (11)$$

$$b = \frac{\sum_{j=1}^{N} P_j - m\sum_{j=1}^{N} T_j}{N} \quad (12)$$

where T_j is the *jth* data point for machine size (in tons), P_j is the corresponding power consumption, and N is the degrees-of-freedom (i.e. number of data points). A similar equation can be formulated using the natural logarithm to linearize the exponential fit. The results of the regression are tabulated in Table 1.

Idle Power	Hold Power	Mold O/C Power
$P = mT + b$	$P = mT + b$	$P = Ae^{BT}$
$m = 0.0269$	$m = 0.0328$	$A = 1.115$
$b = 0.782$	$b = 0$	$b = 0.0066$
$R^2 = 0.98$	$R^2 > 0.99$	$R^2 = 0.99$

Table 1: Regression coefficients for empirical model.

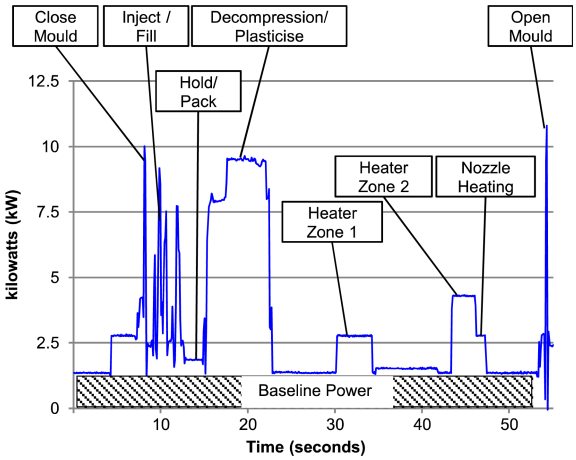

Figure 3: Example power consumption profile [11].

As shown in Table 1, the empirical models fit the data extremely well with the coefficient of determination, R^2, above 0.98 for each model. Despite the high fits, errors in the empirical model are taken into account and are reflected in the outcome. It should be noted that the regression models are valid between 15 to 550 tons due to lack of data at larger machine sizes.

3.3 Cycle Times

In order to calculate the SEC, the power components, detailed in Sections 3.1 and 3.2, are multiplied by their respective cycle times. Note the cycle times in each stage calculated herein are in units of seconds.

The time to inject and fill the sprue, runner, and mold can be approximated using the equation [15]:

$$t_i = 2V_t \frac{dP_t}{P_i} \tag{13}$$

where V_t is the total injected volume, dP_t is the total pressure loss from Equation 3, and P_i is the injection power from Equation 2.

The required time for plasticizing is approximated by the mean residence time, which is the time to plasticize a given shot volume, and can be theoretically determined using the equation [13]:

$$t_r = \frac{HWL_{meter}}{sin\,\bar{\theta} Q_{ex}} \tag{14}$$

where H, W, $\bar{\theta}$, and Q_{ex} are the same parameters as in Equation 5, and L_{meter} is the length of the screw metering section where the large majority of the plasticizing occurs.

The time to pack and hold the molten polymer as well as the time to cool the mold follows the same fundamental conduction heat transfer principle. It is assumed that once the molten polymer in the sprue solidifies the injection unit can be retracted. Therefore, the approximated 1-D heat conduction solution for the hold time is given by [15]:

$$t_h = \frac{\kappa R_s^2}{\pi^2 \alpha} \ln\left[\frac{4(T_i - T_{mo})}{T_x - T_{mo}}\right] \tag{15}$$

where R_s is the sprue radius, α is the average thermal diffusivity of the polymer, T_i is the injection temperature, T_{mo} is the mold temperature, T_x is the polymer melting temperature, and the κ term is a geometric factor, which equals 2/3 for a cylindrical channel. The cooling time, t_{cool}, follows the same equation above with $\kappa = 1$, $T_x = T_{eject}$ (the recommended ejection temperature), and R_s is replaced with h_{max} (the maximum mold wall thickness).

The remaining cycle times involves the mold resetting, which includes movement of the injection unit, mold opening and closing, and part ejection. The resetting time can be approximated using the machine's specified dry cycle time, t_d. However, the reported dry cycle time is typically measured during an empty run with the mold opening and closing at full stroke. Therefore, the dry cycle time can be adjusted to account for actual part sizes, and is estimated using the equation [15]:

$$t_{moc} = 2 + 1.75 t_d \left[\frac{(2D_{mo} + 0.05)}{L_{mo}}\right]^{0.5} \tag{16}$$

where D_{mo} is the part depth and L_{mo} is the maximum clamp stroke. The above equation assumes a 40% opening speed, a part ejection time of 1s, an injection unit travel time of 1s, and a part clearance of 0.05 meters.

Combining Equations 13-16 yields the cycle time. However, as shown in Figure 1, several stages such as holding and plasticizing occur during part cooling. Therefore, to avoid double counting, the actual cycle time is computed as:

$$t_c = t_i + t_{moc} + t_{cool} \qquad \{t_{cool} > t_h + t_r\}$$
$$t_c = t_i + t_h + t_r + t_{moc} \qquad \{otherwise\} \tag{17}$$

3.4 Non-Newtonian Viscosity Model

A unique property of thermoplastic polymers is their viscoelastic behavior, particularly at temperatures above the glass-transition temperature and into the molten state. Unlike Newtonian fluids where the shear stress varies linearly with the shear rate and thus viscosity is constant, the rheological properties of polymer melts vary with shear rate and exhibit "shear thinning" behavior where the viscosity decreases with increasing shear rates [13]. To model the highly nonlinear non-Newtonian viscosity, the four-parameter Carreau Model is used:

$$\frac{\mu(\dot{\gamma}, T) - \eta_\infty}{\eta_o(T) - \eta_\infty} = \frac{1}{\{1 + [\tau(T)\dot{\gamma}]^2\}^{[1-n(T)]/2}} \tag{18}$$

where η_o is the zero shear (or Newtonian) viscosity, η_∞ is the viscosity at infinite shear (assumed to be zero), τ is the relaxation time, n is the Power Law index ($n < 1$ for shear-thinning), and $\dot{\gamma}$ is the shear rate [13]. Each of the parameters (with the exception of η_∞) is dependent on the temperature (and pressure, but assumed to be negligible), where an increase in temperature will decrease the viscosity. At low shear rates the polymer melt behaves more as a Newtonian fluid and is less shear rate dependent as temperature increases.

The for rotational shear done by the screw is used to determine the average shear rates during plasticizing (shear rates during injection are accounted for in Equation 4), and is given as [13]:

$$\dot{\gamma} = \frac{\pi D_b^2 N^2 W \cos\theta_b}{3Q_{ex}} \tag{19}$$

where N, D_b, W, θ_b, and Q_{ex} are the same parameters as in Equation 5. Note that the shear rates during plasticizing are typically lower than that of during injection (same volume at longer processing times) and in some cases may approach that of Newtonian behavior.

4 MODEL PERFORMANCE

Several reported SEC values, publically found in literature, were used to validate the semi-empirical model. Three thermoplastic

polymers, polystyrene (PS), Nylon (PA6), and high-density polyethylene (HDPE), were chosen due to the data availability of their process parameters, and are summarized in Table 2. The parameters for the model are also shown in Tables 3. The process parameters in Table 3 (excluding injection and mold temperature) were adjusted to match the cycle times and throughputs from Table 2. Reasonable dimensional approximations were made based on the description and volume of the part (e.g. a cup modeled as a cylinder with a base).

Material	PS [11]	PA6 [7]	HDPE [3]
Machine Size [tons]	15	75	550
Shot Size [g]	15.6*	880	930
Cycle Time [s]	53.6	30.7	17.7
Throughput [kg/hr]	1.05	10.31	188.66
SEC [MJ/kg]	**9.11**	**2.35**	**2.49**
Part Design	disk	cup	5 gal pail

Table 2: Summary of reported SEC values and respective parameters (*estimated part weight).

Material	PS	PA6	HDPE
Injection Rate [cm^3/s]	40	105	850
RPM	30	150	200
Average Injection Temp	160 [11]	280 [4]	250 [4]
Ejection Temp [C]	80	130	65
Average Mold Temp [C]	20 [11]	90 [4]	27 [4]
Crystallinity	*amorph.*	*semi c.*	*semi c.*

Table 3: Process parameters used in the model.

The process parameters in Tables 2 and 3 were inputted into the model and a Monte Carlo method was used to obtain the mean SEC and 95% confidence interval. The model results for the three polymers are tabulated in Table 4 and plotted in Figure 4. For each material, the reference SEC value from Table 2 is juxtaposed with the model as well as data from two professional material/LCA software databases: Gabi by PE International [16] and CES Selector by Granta Design [17]. For consistency, the same injection molding unit-process module in Gabi was used for all three polymers, while individual datasheets were read from the CES Selector.

As shown in Figure 4, the proposed model performs extremely well, with the reference values well within the 95% confidence interval. The range of the confidence interval, however, is drastically different for polystyrene where the maximum error at 95% confidence is over 23%. This can be attributed its relatively low throughput where the slope of the SEC versus throughput curve is steeper and hence has a higher sensitivity to the cycle time. The higher sensitivity to cycle time is prorogated during the Monte Carlo simulation and thus resulting in a larger relative standard deviation.

	PS	PA6	HDPE
Mean	8.80	2.42	2.39
Standard Deviation	1.057	0.163	0.147
95% Confidence Interval (±)	2.072	0.319	0.288
Relative Error	3.40%	2.98%	4.02%
Confidence Interval Range (±)	23.55%	13.18%	12.05%

Table 4: Model results and errors.

Even with a relatively larger confidence interval range, values from Gabi and CES are clearly seen to differ more significantly. This can be explained by noting the limitations and assumptions of the software. While the injection molding module in Gabi is parametric, the function is a generic linear relation of only to the mass. Hence there is no notion of factoring different machine sizes and throughputs thus giving a higher level of uncertainly. Note that the data given by the software may not necessarily be incorrect since at some particular machine size and throughput the values should be accurate.

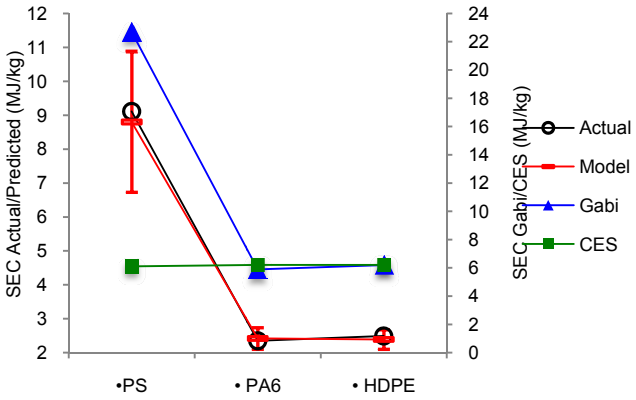

Figure 4: Comparison of model performance.

Figure 5 shows the relative energy breakdown by stage for each of the three polymers. Observe that the contribution of the idle energy decreases with decreasing cycle time (or equivalently increasing throughput). Higher throughput typically implies a shorter cool time since in most cases (depending on the material and part design) cooling is the bottleneck stage. With a shorter cooling time less (baseline) energy is being consumed from simply waiting for the part to cool. Another observation is that the ratio of plasticizing to injection energy is highest in the PA6 case (the injection energy is nearly indistinguishable), which suggests that the heat (temperature) was the dominant means of plasticizing (higher temperature lowers the viscosity). The contribution of the plasticizing and injection energy for the HDPE case is relatively large, which is partially attributed to the high viscosity even at high shear rates.

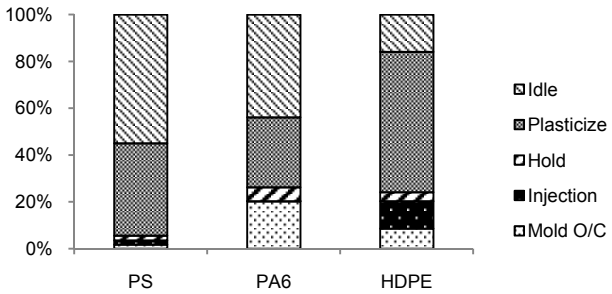

Figure 5: Relative distribution of energy consumption by stage.

5 DISCUSSION OF ERRORS

As with any modeling involving empirical data, especially by means of meta-analysis, errors associated with quality of the data were unavoidable. There were several types of errors involved in this model. The first arise from the extraction of the power consumption values based on images rather than the source data. Due to the limited resolution of the power profile images best estimates of the average power were determined. Additionally, for power consumption profiles where the idling clearly showed discernable

cycling of the heaters (e.g. in Figure 3) the baseline power was used. This was to reduce double counting of the wasted heater power accounted for in Equation 7.

There were also errors due to uncertainty in replicating the processing parameters, machine model, and material (e.g. polymer grade) that were used in creating the original power profiles. Furthermore, approximations in the part dimensions were obviously subject to errors.

Uncertainty and errors in the data were handled using normally distributed probability density functions (PDFs). For data coming from a published source a 2.5% to 5% error was assigned as the standard deviation, while 10% to 15% error was assigned for non-verified data (e.g. part dimensions). Average relative errors were used to represent the standard error in the regression models. The mean values and respective 95% confidence intervals (±1.96 sigma) were determined by using a Monte Carlo technique with an adequate sample size of *N=10,000*.

The final error type was due to the quality of the modeling. Figure 6 below shows the contribution of the total energy calculated by the empirical model vs. the theoretical model. For an instance, the HDPE case shows more sensitivity to the theoretical modeling, which implies that errors from the thermo-mechanical model (i.e. injection and plasticizing) have a greater influence than the errors from the empirical model. In addition, more accurate representation of the material properties, such as having density, specific heat, and thermal conductivity vary as a function of temperature, can improve the accuracy. However, this ratio is highly dependent on the material, process parameters, throughput, etc. as shown when compared to the PA6 case.

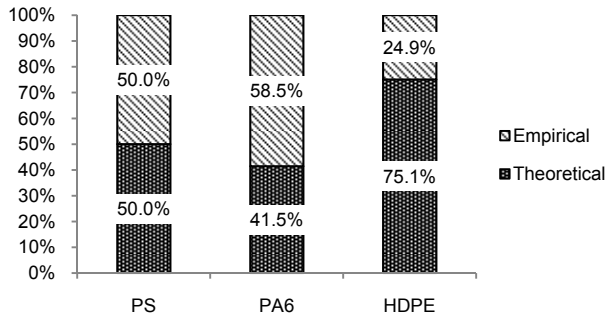

Figure 6: Ratio of empirical to theoretical energy consumption.

6 SUMMARY

This paper presented a detailed semi-empirical model for accurately predicting the electrical energy consumed during injection modeling. The model took into consideration the polymer's rheological non-Newtonian viscoelastic properties and part design while utilizing both thermo-mechanical fundamentals and empirical data. The incorporating the machine specific power characteristic empirical data greatly improved the accuracy of the model. When compared to professional software databases the model performed exceptionally well, particularly when factoring in processing throughput.

Further work is necessary improve the accuracy, particularly the confidence interval range, and robustness of the model. Expansion of the empirical data can included to model machine sizes greater than 550-tons as well as different machine types (e.g. all-electrics), while slight modifications can be made to include non-thermoplastic polymers, such as thermosets and elastomers. Addtional enhancements can be made by adding the power component of a hot runner (not all processes require a hot runner) and by including the energy consumption of any auxiliary equipment such a barrel chiller and dryer for the hopper.

7 REFERENCES

[1] SPI, Inc. (2009): Plastics Fact Sheet, in: www.plasticsdatasource.org, Accessed 11/27/2012.

[2] Barr, D. (2003): Injection Molding Hydraulics the Pressure is Rising, in: Machinery Lubrication { http://www.machinery lubrication.com}, Accessed 11/27/2012.

[3] Thiriez, A. (2006): An Environmental Analysis of Injection Molding, Master Thesis at MIT, Cambridge, MA.

[4] Rosato, D.V., Rosato, D.V., Rosato, M.G. (2000): Injection Molding Handbook, 3rd ed., Kluwer Academic Publishers, Norwell, MA.

[5] Kalla, D., Twomey, J., Overcash, M. (2009): MC2 Injection Molding Process Unit Process Life Cycle Inventory, pp. 1-14, {http://cratel.wichita.edu/uplci/injection-molding/}, Accessed 7/26/2012.

[6] Gutowski, T., Dahmus, J., Thiriez, A. (2006): Electrical Energy Requirements for Manufacturing Processes, in: Proc 13th CIRP Intl Conf LCE, pp. 623-628, Leuven, Belgium.

[7] Ribeiro, I., Peças, P., Henriques, E. (2012): Assessment of Energy Consumption in Injection Molding Process, in: Proc. 19th CIRP Intl Conf LCE, pp. 263-268, Berkeley, California.

[8] Mattis, J., Shen P., DiScipio, W., Leong K. (1996): A Framework for Analyzing Energy Efficient Injection-Molding Die Design, in: Proc 1996 IEEE Intl Symp Elec Env, pp. 207-212 Dallas, Texas.

[9] Gutowski, T., Branham, M.S., Dahmus, J.B., Jones, A.J., Thiriez, A. (2009): Thermodynamic Analysis of Resources Used in Manufacturing Processes, in: Env Sci Tech, Vol. 43, No. 5, pp. 1584-1590.

[10] Duflou, J.R., Kellens, K., Guo, Y., Dewulf, W. (2012): Critical Comparison of Methods to Determine the Energy Input for Discrete Manufacturing Processes, in: CIRP Annals – Mfg Tech, Vol. 61, No.1, pp.63-66.

[11] Qureshi, F., Li, W., Kara, S., Herrmann, C. (2012): Unit Process Energy Consumption Models for Material Addition Processes: A Case of the Injection Molding Process, in: Proc 19th CIRP Intl Conf LCE, pp. 269-274, Berkeley, California.

[12] Weissman, A., Ananthanarayanan, A., Gupta, S.K., Sriram, R.D. (2010): A Systematic Methodology for Accurate Design-Stage Estimation of Energy Consumption for Injection Molded Parts, in: Proc. ASME 2010 IDETC/CIE, pp. 1-13, Montreal, Quebec.

[13] Tadmor, Z., Gogos, C.G. (2006): Principles of Polymer Processing, 2nd ed., Wiley-Interscience, Hoboken, NJ.

[14] Incropera, F.P., DeWitt, D.P., Bergman, T.L., Lavine, A.S. (2007): Fundamentals of Heat and Mass Transfer, 6th ed., John Wiley & Sons, Hoboken, NJ.

[15] Boothroyd, G., Dewhurst, P., Knight, W.A. (2011): Product Design for Manufacture and Assembly, 3rd ed., CRC Press, Boca Raton, FL.

[16] Gabi (Version 5) [Computer Software], PE International, Stuttgart, Germany.

[17] CES Selector 2012 (Version 11.9.9) [Computer Software], Granta Design Limited, Cambridge, United Kingdom.